Isolation and Characterization of a Two-Subunit Cytochrome b – c 1 Subcomplex from Rhodobacter capsulatus and Reconstitution of Its Ubihydroquinone Oxidation (Q o) Site with Purif…

ARTICLE *in* BIOCHEMISTRY · DECEMBER 1998

Impact Factor: 3.02 · DOI: 10.1021/bi981651z · Source: PubMed

5 AUTHORS, INCLUDING:

A. Sami Saribas
Temple University
25 PUBLICATIONS **517** CITATIONS
SEE PROFILE

Brian R Gibney
City University of New York - Brooklyn College
78 PUBLICATIONS **2,927** CITATIONS
SEE PROFILE

Fevzi Daldal
University of Pennsylvania
181 PUBLICATIONS **6,095** CITATIONS
SEE PROFILE

Isolation and Characterization of a Two-Subunit Cytochrome $b-c_1$ Subcomplex from *Rhodobacter capsulatus* and Reconstitution of Its Ubihydroquinone Oxidation (Q_o) Site with Purified Fe-S Protein Subunit†

Maria B. Valkova-Valchanova,‡ A. Sami Saribas,‡ Brian R. Gibney,§ P. Leslie Dutton,§ and Fevzi Daldal*,‡

Department of Biology, Plant Science Institute, and Johnson Research Foundation, Department of Biochemistry and Biophysics, University of Pennsylvania, Philadelphia, Pennsylvania 19104

Received July 10, 1998; Revised Manuscript Received September 15, 1998

ABSTRACT: The presence of a two-subunit cytochrome (cyt) $b-c_1$ subcomplex in chromatophore membranes of *Rhodobacter capsulatus* mutants lacking the Rieske iron−sulfur (Fe-S) protein has been described previously [Davidson, E., Ohnishi, T., Tokito, M., and Daldal, F. (1992) *Biochemistry 31,* 3351−3358]. Here, this subcomplex was purified to homogeneity in large quantities, and its properties were characterized. As expected, it contained stoichiometric amounts of cyt *b* and cyt c_1 subunits forming a stable entity devoid of the Fe-S protein subunit. The spectral and thermodynamic properties of its heme groups were largely similar to those of a wild-type bc_1 complex, except that those of its cyt b_L heme were modified as revealed by EPR spectroscopy. Dark potentiometric titrations indicated that the redox midpoint potential (E_{m7}) values of cytochromes b_H, b_L, and c_1 were very similar to those of a wild-type bc_1 complex. The purified $b-c_1$ subcomplex had a nonfunctional ubihydroquinone (UQH_2) oxidation (Q_o) site, but it contained an intact ubiquinone (UQ) reductase (Q_i) site as judged by its ability to bind the Q_i inhibitor antimycin A, and by the presence of antimycin A sensitive Q_i semiquinone. Interestingly, its Q_o site could be readily reconstituted by addition of purified Fe-S protein subunit. Reactivated complex exhibited myxothiazol, stigmatellin, and antimycin A sensitive cyt *c* reductase activity and an EPR g_x signal comparable to that observed with a bc_1 complex when the Q_o site is partially occupied with UQ/UQH_2. However, a mutant derivative of the Fe-S protein subunit lacking its first 43 amino acid residues was unable to reactivate the purified $b-c_1$ subcomplex although it could bind to its Q_o site in the presence of stigmatellin. These findings demonstrated for the first time that the amino-terminal membrane-anchoring domain of the Fe-S protein subunit is necessary for UQH_2 oxidation even though its carboxyl-terminal domain is sufficient to provide wild-type-like interactions with stigmatellin at the Q_o site of the bc_1 complex.

The ubihydroquinone cytochrome (cyt)[1] *c* oxidoreductase (bc_1 complex) is an integral membrane protein complex, present in a wide range of organisms including bacteria, mitochondria, and chloroplasts (where it is known as the b_6f complex) (for recent reviews, see refs *1*−*5*). It is located in the cytoplasmic membrane, and is a site where energy transduction is coupled to ATP synthesis. In the phototrophic bacterium *Rhodobacter capsulatus*, the bc_1 complex is a key component of both the photosynthetic and respiratory electron-transport chains (*2*, *5*).

R. capsulatus bc_1 complex consists of the cyt *b*, cyt c_1, and Rieske iron−sulfur (Fe-S) protein subunits, which are encoded by the *petABC (fbcFBC)* operon (6), and contains four metal centers. Cyt *b* has two noncovalently bound hemes, b_H and b_L, named after their relatively high (+50 mV) and low (−90 mV) redox midpoint potentials (E_{m7}), respectively (*7*, *8*). Cyt c_1 and the Fe-S protein subunits are attached to the membrane via their carboxyl- and amino-terminal ends, respectively. The carboxyl-terminal domain of the latter subunit contains its [2Fe-2S] cluster (*9*), while the amino-terminal part of the former has a *c*-type heme, and both of these subunits are exposed to the periplasm. The bc_1 complex also contains two ubihydroquinone (UQH_2)/ubiquinone (UQ) binding domains named Q_i and Q_o sites, respectively. The Q_i site is located near the cytoplasmic side of the membrane and catalyzes reduction of UQ, while UQH_2 oxidation takes place at the Q_o site located near the periplasmic side of the membrane (*10*). During recent years a great deal of structural and functional information has been gathered about cyt *b* and its UQ/UQH_2 binding sites from

† This work was supported by NIH Grant GM 38237 to F.D. and by NIH Grant 27309 to P.L.D.

* To whom correspondence should be addressed. Phone: (215) 898-4394. Fax: (215) 898-8780. E-mail: fdaldal@sas.upenn.edu.

‡ Plant Science Institute, University of Pennsylvania.

§ Johnson Research Foundation, University of Pennsylvania.

[1] Abbreviations: cyt, cytochrome; bc_1 complex, ubihydroquinone cyt *c* oxidoreductase; UQH_2, ubihydroquinone; UQ, ubiquinone; Q_o, ubihydroquinone oxidation site; Q_i, ubiquinone reduction site; Fe-S protein, Rieske iron−sulfur protein; [2Fe-2S], two-iron−two-sulfur cluster of the Fe-S protein; EPR, electron paramagnetic resonance; b_L, low-potential *b*-type heme; b_H, high-potential *b*-type heme; E_{m7}, redox midpoint potential at pH 7.0; SDS−PAGE, sodium dodecyl sulfate−polyacrylamide gel electrophoresis; DBH_2, 2,3-dimethoxy-5-decyl-6 methyl-1,4-benzohydroquinone; SHE, standard hydrogen electrode; MOPS, 3-(*N*-morpholino)propanesulfonic acid; PMSF, phenylmethylsulfonyl fluoride; DDM, dodecyl maltoside; DMSO, dimethyl sulfoxide; EDTA, ethylenediaminetetraacetic acid; PMS, *N*-methyldibenzopyrazine methosulfate; PES, *N*-ethyldibenzopyrazine ethosulfate; DAD, 2,3,5,6-tetramethyl-1,4-phenylenediamine.

10.1021/bi981651z CCC: $15.00
Published on Web 10/26/1998

studies of inhibitor-resistant or nonfunctional mutations located in the bc_1 complex (*11*−*13*). These studies have revealed a low-resolution topology of these sites which is now largely confirmed by the recent determination of the three-dimensional structure of various mitochondrial bc_1 complexes (*14*, *15*). The available structures have established the distances between the redox centers of the bc_1 complex and the overall organization of the subunits. Moreover, the different forms of crystals obtained using bc_1 complexes purified from different species revealed that while the distances between the cyt c_1 and cyt *b* heme groups remain constant those of the [2Fe-2S] cluster to cyt b_L and cyt c_1 vary considerably (*15*). This finding suggested that the Fe-S protein may be mobile enough to yield different forms of crystals in which it occupies distinct positions with respect to the other subunits of the bc_1 complex. Whether the proposed mobility of the Fe-S protein subunit is an intrinsic component of Q_o site catalysis remains to be seen.

Our earlier work has indicated that *R. capsulatus* mutants affecting the universally conserved cysteine and histidine ligands of the [2Fe-2S] cluster of the Fe-S protein subunit produce large amounts of cyt *b* and cyt c_1 while they completely lack the Fe-S protein subunit (*16*). In chromatophore membranes of such mutants, apparently cyt *b* and cyt c_1 recognize each other to form a two-subunit complex with an intact Q_i site and an inactive Q_o site (*17*). Purification of this $b-c_1$ subcomplex was therefore attempted in order to prove that these subunits indeed form a subcomplex in the absence of the Fe-S protein. Here we report the isolation and detailed characterization of a stable, two-subunit $b-c_1$ subcomplex from *R. capsulatus*. We demonstrate for the first time for a bacterial bc_1 complex that the purified $b-c_1$ subcomplex can regain its cyt *c* reductase activity upon addition of purified Fe-S protein subunit in vitro provided that the amino-terminal membrane anchor of this subunit is intact. Moreover, we show that in the presence of the Q_o site inhibitor stigmatellin a soluble derivative of the Fe-S protein subunit lacking the membrane anchor can reconstitute a stigmatellin-inhibited Q_o site. The overall findings therefore establish that the amino-terminal membrane anchor of the Fe-S protein subunit is required for the formation of an active Q_o site, even though its [2Fe-2S]-carrying carboxyl-terminal portion is sufficient to interact with cyt *b* appropriately in the presence of stigmatellin. The availability of a reconstitutively active $b-c_1$ subcomplex coupled with an easy in vitro reconstitution assay should be very useful in dissecting the mechanism of UQH_2 oxidation at the Q_o site of the bc_1 complex.

MATERIALS AND METHODS

Bacterial Strains and Growth Conditions. The *R. capsulatus* strains pMTS1/MT-RBC1 overproducing the wild-type bc_1 complex (*18*), pF:H135L/MT-RBC1 lacking the Fe-S protein subunit and overproducing the cyt $b-c_1$ subcomplex (*16*), and pB:(T163F+G182S)/MT-RBC1 producing a soluble form of the Fe-S protein subunit (*19*) have been described previously. These strains were grown chemoheterotrophically in a "mixed medium" [1 volume of medium A (*20*) + 1 volume of MPYE (*6*)] containing 0.625 μg/mL tetracycline [pF:H135L/MT-RBC1 and pB:(T163F+G182S)/MT-RBC1] or 10 μg/mL kanamycin (pMTS1/MT-RBC1) either in 2 L flasks using a rotary shaker at 150 rpm or in 20 L carboys under semiaerobic conditions. Under the conditions used here, the typical biomass yield was about 3−4 g of cells (wet weight) per liter of growth medium.

Purification of Wild-Type bc_1 Complex and $b-c_1$ Subcomplex. The bc_1 complex and $b-c_1$ subcomplex were isolated from chromatophore membranes by a variation of the procedure described in (*8*). Chromatophore membranes were obtained from frozen cell paste after two passages through a French pressure cell according to (*21*) and either used immediately or stored frozen at −80 °C. They were resuspended to a final protein concentration of 10 mg/mL in 50 mM Tris-HCl buffer, pH 8.0, containing 100 mM NaCl, 20% glycerol, 1 mM PMSF, and 1 mM EDTA. Dodecyl maltoside (DDM, 20% w/v stock) was added dropwise to this suspension to a final concentration of 1 mg/mg of total protein. The mixture was stirred for 45 min at 4 °C, and then centrifuged at 120000*g* for 90 min. The supernatant was collected, adjusted to pH 8.0, and loaded onto a DEAE-BioGel A column (2.6 × 55 cm) previously equilibrated with 50 mM Tris-HCl, pH 8.0, 20% glycerol, and 100 mM NaCl (equilibration buffer). The column was washed first with 2−3 bed volumes of equilibration buffer containing 0.01% (w/v) dodecyl maltoside, followed by 5−6 bed volumes of the same buffer containing 150 mM NaCl. These washes removed large amounts of photosynthetic pigments as well as the cbb_3-type cyt *c* oxidase (*22*). The adsorbed wild-type bc_1 complex, or the $b-c_1$ subcomplex, was eluted with 3 bed volumes of a linear 150−400 mM NaCl gradient. For the bc_1 complex, fractions containing the highest DBH_2:cyt *c* reductase activity were pooled. In the case of the $b-c_1$ subcomplex, fractions were monitored for their absorption at 280 and 420 nm, and for their dithionite-reduced *minus* ferricyanide-oxidized optical difference spectra at 500−600 nm, and those containing the highest concentrations of cyt *b* and cyt c_1 were pooled. Under the conditions used, both the bc_1 complex and the $b-c_1$ subcomplex were typically eluted between 230 and 270 mM NaCl concentrations. The pooled fractions were dialyzed against the equilibration buffer without glycerol, and concentrated using an Amicon Diaflo apparatus and a PM30 membrane. The concentrated sample (25−30 mL) was applied onto a DEAE-Fractogel (Toyopearl 650) column (2.6 × 17 cm) equilibrated with the equilibration buffer without glycerol but containing 0.01% (w/v) DDM. The column was washed with 3 bed volumes of equilibration buffer containing 150 mM NaCl, and eluted with 3 bed volumes of a linear 150−400 mM NaCl gradient in the same buffer. Fractions containing the bc_1 complex or the $b-c_1$ subcomplex were pooled, concentrated as above using a PM30 membrane, and stored at −80 °C.

Purification of the Fe-S Protein Subunit from the Wild-Type bc_1 Complex and Its Reconstitution to the Purified $b-c_1$ Subcomplex. Reconstitutively active *R. capsulatus* Fe-S protein was obtained from purified bc_1 complex using Phenyl Sepharose chromatography according to (*23*) for *R. sphaeroides*, except that in the case of *R. capsulatus* 2% sodium cholate was required for the dissociation of the Fe-S protein subunit from the bc_1 complex. The purified $b-c_1$ subcomplex was reconstituted in vitro with purified Fe-S protein essentially as described by (*24*) with the following modifications. The *R. capsulatus* $b-c_1$ subcomplex (1.12 nmol) was mixed with 275 μg of lecithin and varying amounts of

purified Fe-S protein, and the final volume was brought to 150 μL with 40 mM potassium phosphate buffer, pH 7.4 containing 0.5 mM EDTA. This mixture was incubated for 1 h at 35 °C, then diluted 2-fold with 50 mM Tris-HCl, pH 8.0, buffer containing 100 mM NaCl and 0.01% (w/v) DDM, and centrifuged at 220000*g* for 4 h. This treatment, which pelleted the reconstituted bc_1 complex and left the unbound Fe-S protein in the supernatant, was repeated twice and the pellet resuspended in the same buffer to a final concentration of 40−45 μM cyt c_1. The DBH_2:cyt *c* reductase activity was measured essentially as described earlier (*21*) but in the presence of 0.02% Tween 20. The assay mixture (2 mL total volume) contained 40 mM phosphate buffer, pH 7.4, 0.5 mM EDTA, 250 μg of lecithin, 0.02% Tween 20, and 50 μM horse heart cyt *c*. The DBH_2 was added to a concentration of 40 μM from a DMSO stock solution, and non enzymatic reduction of cyt *c* was followed at 550 nm with a Hitachi U-3200 spectrophotometer. The reaction was initiated by adding the enzyme, and the rate of cyt *c* reduction monitored at 550 nm was determined using an extinction coefficient ϵ_{550} of 18.5 mM^{-1} cm^{-1} (*25*). The DBH_2-dependent cyt *c* reductase activity sensitive to the bc_1 complex inhibitors myxothiazol, stigmatellin, and antimycin A was taken as an indication of the reactivation of the $b-c_1$ subcomplex.

For EPR analysis, the reconstitution assay was scaled up by about 10-fold so that 14 nmol of purified b-c_1 subcomplex was incubated with 10 nmol of purified Fe-S protein and treated as above. Small aliquots of the reconstituted subcomplex were used for SDS−PAGE and DBH_2:cyt *c* reductase activity analyses. The remainder of the sample was prepared for EPR spectroscopy and its EPR spectrum recorded as described earlier (*26*).

Reconstitution of the $b-c_1$ Subcomplex with a Soluble Form of the Fe-S Protein. For this purpose, highly concentrated membrane-free chromatophore supernatants of the double mutant pB:(T163F+G182S)/MT-RBC1 producing a soluble form of the Fe-S protein subunit (*19*) were used. The concentrated supernatants (18 mg/mL) were divided into two 300 μL portions, to one of which stigmatellin was added to a final concentration of 40 μM. They were then mixed with the $b-c_1$ subcomplex (14 nmol) and lecithin (275 μg) and incubated for 1 h at 35 °C. Small aliquots were taken to measure the DBH_2:cyt *c* reductase activity (*21*), the remainder of the samples was reduced with 20 μM sodium ascorbate, and their EPR spectra were recorded as described previously (*26*).

Spectroscopy. Optical spectra were obtained using a Hitachi U-3200 spectrophotometer with a 1 cm light path cuvettes. Cyt c_1 content was calculated from ascorbate-reduced *minus* ferricyanide-oxidized optical difference spectra using an extinction coefficient $\epsilon_{551-542}$ of 20 mM^{-1} cm^{-1} (*27*). Cyt *b* content was calculated from dithionite-reduced *minus* ascorbate-reduced optical difference spectra using an extinction coefficient $\epsilon_{560-574}$ of 28 mM^{-1} cm^{-1} (*28*). Dark potentiometric titrations of the $b-c_1$ subcomplex, and the wild-type bc_1 complex, were carried out according to (*29*), using a double-beam spectrophotometer (University of Pennsylvania Instrumentation Group) fitted with an anaerobic redox cuvette. Mediation between the electrodes, solution, and redox centers was achieved using a collection of redox mediator dyes chosen for their electrochemical potentials and their lack of optical interference in the 500−600 nm region. For these experiments, the total bc_1 complex, or the $b-c_1$ subcomplex, was adjusted to a protein concentration of 2−3 μM in 50 mM MOPS, 100 mM KCl buffer, pH 7.0, in the presence of the following mediators: *N*-methyldibenzopyrazine methosulfate (PMS), *N*-ethyldibenzopyrazine ethosulfate (PES), 1,4-naphthoquinone, 1,2-naphthoquinone, and 2-hydroxy-1,4-naphthoquinone at 25 μM each and 50 μM 2,3,5,6-tetramethylphenylenediamine (DAD). Spectra were taken at E_h intervals of 5−20 mV during a reductive titration, and the spectral data thus acquired were manipulated using the Labview software program (National Instruments) developed for this spectrophotometer by Dr. H. Ding. The optical spectra of the individual hemes b_H, b_L, and c_1 were derived from the titration data using appropriate E_h cuts.

The antimycin A induced shift of the cyt *b* absorption spectrum was recorded with a Beckman DU640 spectrophotometer using 2.5 μM bc_1 complex, or $b-c_1$ subcomplex, resuspended in 50 mM Tris-HCl, pH 8.0, buffer containing 100 mM NaCl and 0.01% (w/v) DDM. Samples were first reduced with dithionite, and base lines were recorded; then antimycin A was added to a final concentration of 30 μM from a stock solution in DMSO, and the reduced plus antimycin A *minus* reduced spectra were recorded between 400 and 600 nm.

EPR spectra were obtained using a Bruker Model ESP-300 E EPR spectrometer, equipped with a helium cryostat. The experimental conditions were as described earlier (*8*, *26*), and are given in the legends of the corresponding figures.

Other Assays and Analytical Measurements. Protein concentrations were determined by the method of Lowry et al. (*30*), using bovine serum albumin as a standard. One-dimensional SDS−PAGE was performed according to Laemmli (*31*) using a 15% linear gel. For immunoblot analyses, gels were blotted onto Immobilon-P membranes (Millipore) (*32*), and monoclonal antibodies raised against the subunits of the bc_1 complex from *R. capsulatus* (*21*) were used as immunoprobes. Goat anti-mouse IgG conjugated to horseradish peroxidase was used as a secondary antibody, and detection of the antigen−antibody immunocomplex was enhanced using 3,3′-diaminobenzidine tetrachloride in the presence of 0.12% $NiCl_2$.

The UQ content of the purified $b-c_1$ subcomplex was determined as described by (*33*). Briefly, 36 nmol of purified $b-c_1$ subcomplex in 50 mM Tris-HCl, pH 8.0, buffer, containing 100 mM NaCl and 0.01% (w/v) DDM, was extracted with a 10-fold excess of acetone/methanol (1/1, v/v) mixture. The mixture was shaken gently for 10 min, followed by the addition of an equal volume of petroleum ether. The latter solvent containing UQ was collected, washed with 95% (v/v) methanol, and evaporated. The dried extract was dissolved in ethanol and the UQ amount determined using borohydride reduced *minus* ferric chloride oxidized absorption difference spectra and an ϵ_{275} of 14 mM^{-1} cm^{-1}.

Chemicals. DEAE-BioGel A and DEAE-Fractogel (Toyopearl-650) were obtained from BioRad and EM Separation Technology, respectively. Dodecyl maltoside was purchased from Anatrace Inc., and lecithin, Tween 20, horse heart cytochrome *c*, PMS, PES, and antimycin were obtained from Sigma. Myxothiazol was purchased from Boehringer-Mannheim Biochemicals, and 2-hydroxy-1,4-naphthoquinone

Table 1: Purification of *R. capsulatus* $b-c_1$ Subcomplex from a Mutant Lacking the Fe-S Protein and Its Comparison to the Wild-Type bc_1 Complex

(A) Purification of $b-c_1$ Subcomplex							
		cyt *b* (nmol)		cyt *c* (nmol)			
step	protein (mg)	per mg of protein	total	per mg of protein	total	yield (%)	purification (*x*-fold)
chromatophores + DDM	1740	1.20	2088	1.25	2175		
DDM extract	1582	1.26	2192	1.27	2009	100.0	−
DEAE-BioGel A pool	100	12.30	1230	8.90	890	6.3	10
concentrated pool applied on Fractogel	60	13.00	780	9.30	558	3.8	10.3
Fractogel pool	43	15.40	662	10.80	464	2.7	12.2
PM30K concentrate	30	15.80	474	11.00	330	1.9	12.5

(B) Comparison of $b-c_1$ Subcomplex to bc_1 Complex			
	cyt *b* content[a]	cyt *c* content[a]	DBH_2−cyt *c* reductase activity[b]
$b-c_1$ subcomplex	15.8	11.0	0
bc_1 complex	22.0	15.0	41.0

[a] Nanomoles per milligram of protein. [b] Antimycin A sensitive activity (micromoles of cyt *c* reduced per milligram of protein per minute).

and 2,3,5,6-tetramethyl-1,4-phenylenediamine (DAD) were from Aldrich. All other chemicals were of reagent grade or of highest quality commercially available.

RESULTS

Purification of the $b-c_1$ Subcomplex. The $b-c_1$ subcomplex was purified essentially as described for the wild-type bc_1 complex (*8*). This procedure yielded about 30 mg of highly pure $b-c_1$ subcomplex starting with approximately 1.5 g of chromatophore membranes prepared using 165 g of cells (wet weight). The only contaminants in the final preparations of the $b-c_1$ subcomplex, and also the bc_1 complex, were about 5−10% of photosynthetic pigments associated with the light-harvesting complexes I and II. A comparison of the composition and enzymatic activity of purified $b-c_1$ subcomplex and bc_1 complex is presented in Table 1. Cyt *b* and cyt c_1 contents (15.8 and 11.0 nmol/mg of protein, respectively) of the $b-c_1$ subcomplex are about 30% less than those of the wild-type bc_1 complex (22 and 15 nmol/mg of protein, respectively) although the cyt *b* to cyt c_1 ratios (approximately 1.45 to 1.50) are similar in both cases. Assuming that the two preparations are of similar purity, this difference suggests that the $b-c_1$ subcomplex is more prone to loss of its prosthetic groups during purification. As expected, the purified $b-c_1$ subcomplex exhibited no detectable DBH_2-dependent antimycin A sensitive cyt *c* reductase activity while the purified bc_1 complex had high DBH_2:cyt *c* reductase activity [about 41 μmol of horse heart cyt *c* reduced (mg of protein)$^{-1}$ min^{-1}], which was completely inhibited by antimycin A (Table 1).

SDS−PAGE analysis of purified wild-type bc_1 complex revealed three major bands with molecular masses of 41, 31, and 24 kDa corresponding to cyt *b*, cyt c_1, and the Fe-S protein subunits, respectively (Figure 1A). In contrast, the purified $b-c_1$ subcomplex contained only two major bands with molecular masses of 41 and 31 kDa. Furthermore, immunoblot analysis using specific monoclonal antibodies revealed that the 24 kDa Fe-S protein subunit is completely absent in the $b-c_1$ subcomplex preparation (Figure 1B). The additional bands of higher molecular mass seen both with the bc_1 complex and with the $b-c_1$ subcomplex correspond to their aggregated forms as observed previously (*8*). The high purity of $b-c_1$ subcomplex prepared by the protocol used here was indicated by the high cytochrome content and

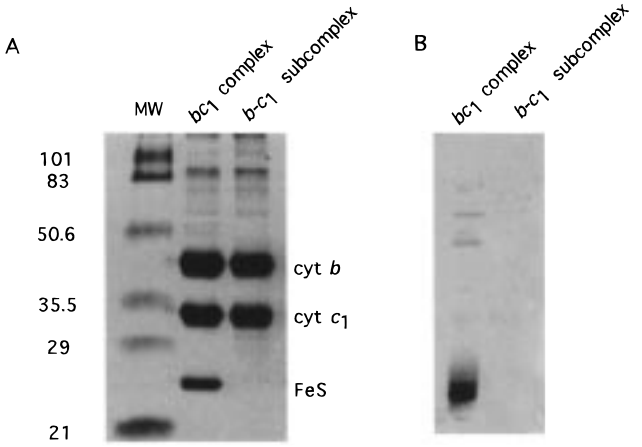

FIGURE 1: SDS−PAGE and immunoblot analyses of purified bc_1 complex and purified $b-c_1$ subcomplex. Panel A: Approximately 4 μg of total protein was used in each case, and the gel was stained with Coomassie Brilliant Blue. Panel B: A gel identical to that shown in panel A was blotted into a PVDF membrane and probed with monoclonal antibodies specific for *R. capsulatus* Fe-S protein.

SDS−PAGE patterns, as well as by a high absorption ratio (0.92) of the 411 to 280 nm peaks of the oxidized $b-c_1$ subcomplex (data not shown).

Spectral Properties and Electrochemistry of the Redox Centers. The $b-c_1$ subcomplex isolated from *R. capsulatus* displayed an optical spectrum characteristic of the bc_1 complexes isolated from other sources (*34*). Its oxidized spectrum has a Soret absorption peak at 411 nm, and the dithionite-reduced spectrum α absorption bands at 553 and 558.5 nm, β absorption bands at 523.5 and 529 nm, and a Soret band at 426.5 nm (data not shown). These peak values were essentially the same as those observed with a wild-type bc_1 complex (*8*).

The effect of the absence of the Fe-S subunit protein on the spectral and thermodynamic properties of the redox centers b_H, b_L, and c_1 was tested by comparison of the $b-c_1$ subcomplex with the wild-type bc_1 complex. The redox midpoint potential (E_{m7}) values of the individual hemes centers were determined by dark equilibrium titration (Figure 2). In the $b-c_1$ subcomplex, cyt b_H and b_L titrated with E_{m7} values of 35 and −130 mV while in the wild-type bc_1 complex they titrated with E_{m7} values of 43 and −138 mV, respectively. Thus, within the limits of experimental errors (±15 mV), no significant difference in the E_{m7} values of

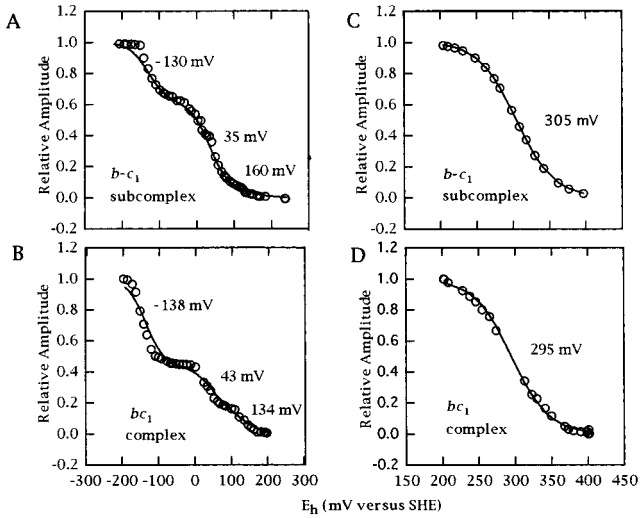

FIGURE 2: Dark equilibrium redox titrations of cyt *b* and cyt c_1 subunits of purified $b-c_1$ subcomplex and bc_1 complex. Absorption of the *b*-type hemes of the $b-c_1$ subcomplex (1.5 μM) (panel A) and the bc_1 complex (1.6 μM) (panel B) was monitored at 560−540 nm as a function of ambient E_h. The data obtained were fit using three $n = 1$ components, and the E_{m7} values thus obtained are indicated. The wavelength pair 551.2−536 nm was used to titrate the *c*-type hemes of purified $b-c_1$ subcomplex (1.5 μM) (panel C) and purified bc_1 complex (1.6 μM) (panel D). The data obtained were fit using one $n = 1$ component, and the E_{m7} values thus obtained are indicated.

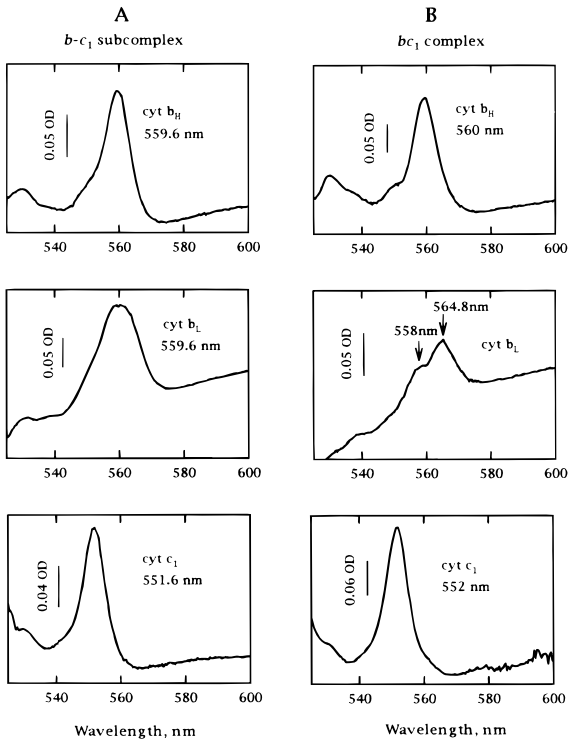

FIGURE 3: Reduced *minus* oxidized optical absorption spectra of cytochromes b_H, b_L, and c_1 of purified $b-c_1$ subcomplex and purified $b-c_1$ complex. The spectra were derived from the data obtained during the redox titrations shown in Figure 2 using appropriate E_h values as follows for $b-c_1$ subcomplex (panel A) and bc_1 complex (panel B), respectively: cyt b_H, 10 *minus* 200 mV and 2 *minus* 190 mV; cyt b_L, −188 *minus* −24 mV and −187 *minus* −15 mV; cyt c_1, 202 *minus* 401 mV and 200 *minus* 407 mV. Note the modified cyt b_L spectrum of the purified $b-c_1$ subcomplex.

cyt b_H and b_L between the $b-c_1$ subcomplex and the bc_1 complex was observed. A third component referred to as cyt b_{150} (*18*, *35*, *36*) was also detectable, and E_{m7} values of 160 mV for the $b-c_1$ subcomplex and 134 mV for the bc_1 complex were used to obtain the best fit to the experimental data shown in Figure 2. Finally, for cyt c_1 subunit, very similar E_{m7} values for the $b-c_1$ subcomplex (305 mV) and the bc_1 complex (295 mV) were observed.

When the optical spectra of cytochromes b_H, b_L, and c_1 were compared, no significant differences were detected in the absorption maxima of cyt b_H and cyt c_1 between the $b-c_1$ subcomplex and the bc_1 complex. However, the optical spectrum of the $b-c_1$ subcomplex was clearly modified (Figure 3, panels A and B). While cyt b_L of a wild-type bc_1 complex had a typical split α-peak spectrum (558 and 564.8 nm), that of the $b-c_1$ subcomplex displayed a single broad peak with a maximum around 559.6 nm. Considering that in the chromatophore membranes (*17*), and also following the BioGel chromatography step (data not shown), cyt b_L of the $b-c_1$ subcomplex still exhibited its typical split α peak, this finding together with the lower content of total cyt *b* in the purified $b-c_1$ subcomplex suggested that the conformation of cyt b_L was modified, and part of it was lost, during the final steps of purification and storage.

EPR Characteristics of Cyt b Hemes of the Isolated $b-c_1$ Subcomplex. The low-spin cyt *b* hemes of the bc_1 complex exhibit unusual EPR spectra (*35*), and their g_z values (3.78 and 3.45 for cyt b_L and cyt b_H, respectively) are known. Thus, the EPR characteristics of the cyt b_H and b_L of isolated $b-c_1$ subcomplex and bc_1 complex were compared to further assess the extent of the perturbation detected by optical spectroscopy. While the cyt *b* hemes of the purified $b-c_1$ subcomplex, and the bc_1 complex, have similar g_z signals [$g_z = 3.79$ for cyt b_L and 3.46 for cyt b_H], on the other hand, the overall line shape of the EPR spectrum obtained using the $b-c_1$ subcomplex was modified (Figure 4) by a signal with a g_z value of 3.69. This EPR resonance, observed in the $b-c_1$ subcomplex spectrum, indicates that the conformation of a large portion of the cyt b_L heme was modified. Finally, a significant amount of an EPR signal at a $g = 6$ value corresponding to a high-spin heme was also detected in both the $b-c_1$ subcomplex and the bc_1 complex (data not shown), as previously reported for the bc_1 complex from *R. sphaeroides* (*37*).

UQ Content and the Q_i Site of Isolated $b-c_1$ Subcomplex. UQ content of the purified $b-c_1$ subcomplex was determined as described under Materials and Methods to assess the occupancy of its Q binding sites. It contained about 0.5 nmol of UQ/nmol of cyt c_1, a value which is within the same range determined previously (0.5−3.0 UQ/c_1) for a purified wild-type bc_1 complex (*8*). Thus, the $b-c_1$ subcomplex isolated here was similar to a wild-type bc_1 complex with the lowest UQ content. However, because of the absence of the Fe-S protein subunit, it was not possible to assess to what extent the UQ molecules present in the purified $b-c_1$ subcomplex were associated with its inactive Q_o site.

The intactness of the Q_i site of the purified $b-c_1$ subcomplex and its UQ content were probed using antimycin A. This inhibitor binds nearby the Q_i site (*14*, *15*), and induces a shift in the optical spectrum of cyt b_H (*38*, *39*). The antimycin A induced spectral shift observed with the $b-c_1$ subcomplex was similar to that exhibited by a wild-type bc_1 complex, with minima at 421 and 555 nm and

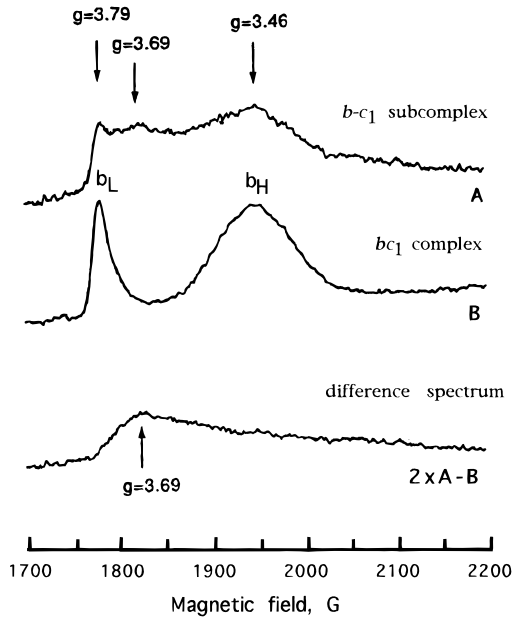

FIGURE 4: EPR spectra of the *b*-type cytochromes of the purified $b-c_1$ subcomplex (A) and bc_1 complex (B). The spectrum $2\times A - B$ corresponds to the spectrum obtained by subtracting arithmetically the spectrum of the bc_1 complex from that of $b-c_1$ subcomplex multiplied by 2. The $b-c_1$ subcomplex (120 μM) and bc_1 complex (100 μM) were reduced with 40 μM ascorbate and rapidly frozen in liquid nitrogen. EPR spectra were taken under the following conditions: temperature, 10 K; microwave frequency, 9.4 GHz; microwave power, 5 mW; modulation amplitude, 12.5 G; modulation frequency, 100 kHz.

maxima at 560 nm (Figure 5A with inset). Thus, antimycin A binds to the isolated $b-c_1$ subcomplex in a way similar to the wild-type bc_1 complex.

Finally, the functional intactness of the Q_i site of the $b-c_1$ subcomplex was also probed by monitoring its antimycin A sensitive, ubisemiquinone radical signal at $g = 2.005$ using EPR spectroscopy. Upon addition of this inhibitor to the purified $b-c_1$ subcomplex, the antimycin A sensitive ubisemiquinone radical disappeared in a manner similar to that observed with the wild-type bc_1 complex (8) (Figure 5B). The data indicated that at least a fraction of the UQ detected in the purified $b-c_1$ subcomplex was associated with its Q_i site which was able to generate a stable Q_i ubisemiquinone radical like the wild-type bc_1 complex.

Reconstitution of UQH_2 Oxidation Activity of the Isolated Inactive $b-c_1$ Subcomplex with Purified Fe-S Protein Subunit. Incubation of purified $b-c_1$ subcomplex and the Fe-S protein subunit at 35 °C as described under Materials and Methods led to the recovery of the DBH_2-dependent cyt *c* reductase activity of the $b-c_1$ subcomplex (Figure 6). The amount of recovered activity increased as a function of the amount of Fe-S protein subunit added. The highest activity was reached at a ratio of 1 mol of Fe-S protein subunit to 1.3 mol of purified $b-c_1$ subcomplex. The recovered activity [approximately 0.32 μmol of cyt *c* reduced min^{-1} (mol of cyt $c_1)^{-1}$ or 10.2 μmol of cyt *c* reduced min^{-1} (mg of protein)$^{-1}$] amounted to approximately 25% of that of the wild-type bc_1 complex, and was inhibited completely by addition of antimycin A and myxothiazol (Figure 6, inset). Additional proof that the recovered DBH_2:cyt *c* reductase activity was indeed due to reconstitution of the purified Fe-S protein subunit to the $b-c_1$ subcomplex was obtained by SDS−PAGE and EPR analyses. The presence of the 24 kDa Fe-S polypeptide, which was undetectable previously in the purified $b-c_1$ subcomplex (Figure 1), became evident upon reconstitution (Figure 7, panel A). Similarly, the EPR $g_y = 1.90$ and $g_x = 1.80$ signals which were absent in the EPR spectrum of the $b-c_1$ subcomplex (Figure 7, panel B, trace B) became comparable to that of the bc_1 complex (trace A). The shift of the Fe-S protein subunit $g_x = 1.80$ signal from 1.765 to 1.800 in the reconstituted $b-c_1$ subcomplex suggested that the Q_o site of the reconstituted sample was competent to bind UQ/UQH_2 appropriately, although it was partially empty (*33*).

The Amino-Terminal Anchor Domain of the Fe-S Protein Subunit Is Required for the Reconstitution of the Q_o Site of the $b-c_1$ Subcomplex. Very recently, we have described a *R. capsulatus* mutant which produces a soluble form of the Fe-S protein subunit via proteolytic cleavage at its amino-terminal position 44 (*19*). This soluble derivative of the Fe-S protein subunit has an intact [2Fe-2S] cluster with an E_{m7} value similar to that of a wild-type complex even though it is no longer anchored to the membrane. The availability of this mutant provided us the opportunity to probe the role of the amino-terminal membrane anchor to the Fe-S protein subunit for its binding to the Q_o site of the bc_1 complex. Thus, chromatophore membrane supernatants containing a soluble form of the Fe-S protein subunit prepared as described in (*19*) were used to reconstitute the $b-c_1$ subcomplex. However, no DBH_2:cyt *c* reductase activity was recovered under the same experimental conditions which fully restored the activity of $b-c_1$ subcomplex when an intact Fe-S protein subunit was used. Furthermore, additional proof that the soluble derivative of the Fe-S protein could not reconstitute the Q_o site of $b-c_1$ subcomplex was obtained by EPR spectroscopy. Like the purified Fe-S protein, the soluble derivative also had no pronounced EPR $g_x = 1.80$ signal, and it did not respond to the addition of stigmatellin (Figure 8, traces A and B), as described previously for the bovine (*40*) and *R. capsulatus* (*19*) soluble Fe-S protein subunits. Unlike with the intact Fe-S subunit (Figure 7), this EPR g_x signal was not restored when the $b-c_1$ subcomplex was incubated with the soluble form of the Fe-S protein subunit (Figure 8, trace D). Thus, the amino-terminal anchor of the Fe-S protein is required for the reconstitution of a catalytically active Q_o site of the bc_1 complex.

Next, considering that the carboxyl-terminal portion of the Fe-S protein subunit carrying the [2Fe-2S] cluster interacts closely with cyt *b* at the Q_o site, as revealed by the very recent genetic (*41*) and structural (*15*) studies, we postulated that stigmatellin would mediate binding of the soluble Fe-S protein subunit into the Q_o site. Indeed, when the $b-c_1$ subcomplex was incubated with the soluble form of the Fe-S protein subunit in the presence of stigmatellin, an EPR $g_x = 1.782$ signal identical to that observed with a wild-type bc_1 complex in the presence of this inhibitor was obtained (Figure 8, trace E). Thus, the soluble form of the Fe-S protein subunit can occupy the Q_o site of the $b-c_1$ subcomplex at a position similar to that of the intact Fe-S protein in the presence of stigmatellin. Therefore, the overall data revealed that for reconstitution of a catalytically active Q_o site, at least two interaction points, one provided by the amino-terminal anchor and the other by the carboxyl-terminal domain of the Fe-S protein, are necessary.

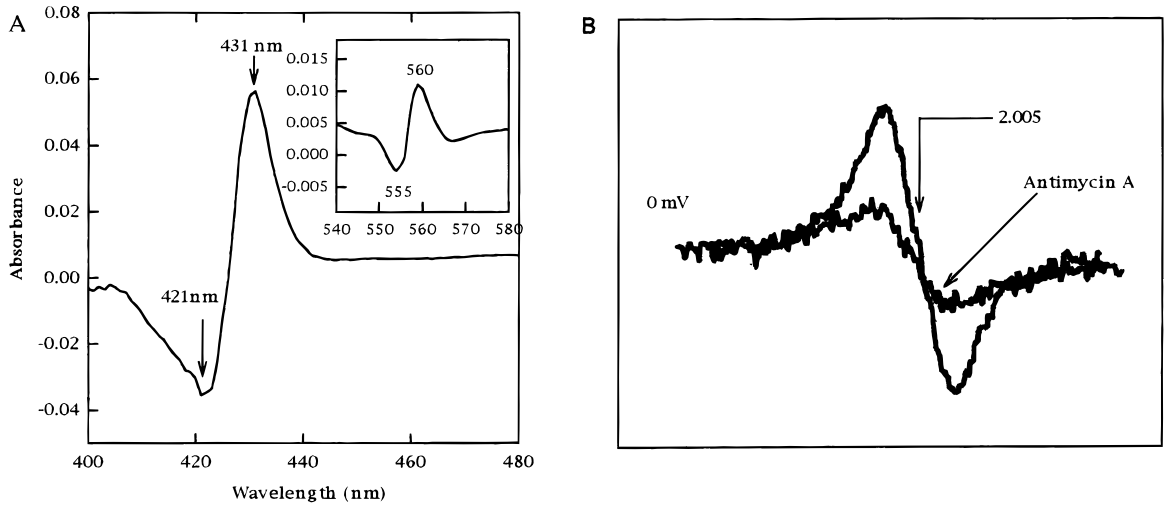

FIGURE 5: Antimycin A induced spectral shift of reduced cyt b_H of purified $b-c_1$ subcomplex (panel A). The inset depicts the 540−580 nm region of the spectra obtained using the same samples. The effect of antimycin A on the EPR $g = 2.0$ radical signal exhibited by the purified $b-c_1$ subcomplex is shown in panel B. The $b-c_1$ subcomplex (53 μM) was suspended in 50 mM Bis-Tris buffer, pH 9.0, and reduced with dithionite to an E_h value of 0 mV. The sample was rapidly frozen, and EPR spectra were taken under the following conditions: temperature, 100 K, microwave frequency, 9.25 GHz; microwave power, 0.5 mW; modulation amplitude, 5 G; modulation frequency, 100 kHz. After recording this spectrum, the sample was thawed, antimycin A was added to a final concentration of 10 μM, the sample was frozen, and its EPR spectrum was re-recorded.

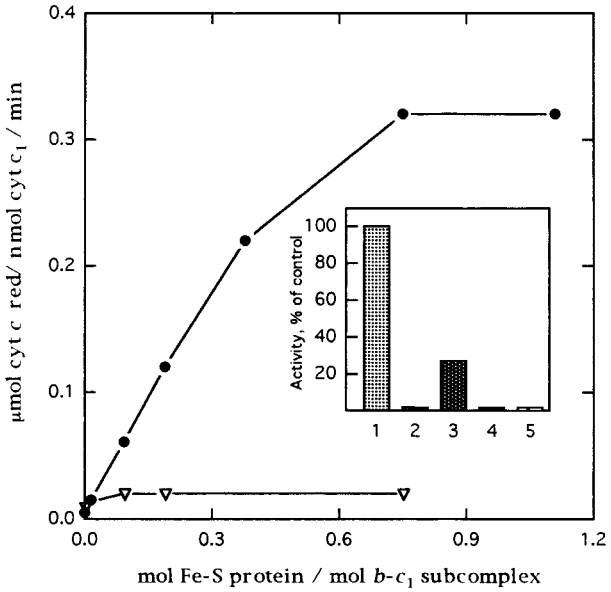

FIGURE 6: Reconstitution of the cyt *c* reductase activity of the purified $b-c_1$ subcomplex. Various amounts of purified Fe-S protein were incubated with 1.12 nmol of purified $b-c_1$ subcomplex in the absence (●) and in the presence (▽) of 0.2 μmol of antimycin A per milligram of protein, and DBH_2-dependent cyt *c* reductase activity was measured as described under Materials and Methods. The inset shows the DBH_2:cyt *c* reductase activity obtained under the same conditions, using (1) purified bc_1 complex, (2) purified $b-c_1$ subcomplex, (3) purified $b-c_1$ subcomplex reconstituted with the Fe-S protein subunit (1 mol of Fe-S protein/1.3 mol of $b-c_1$ subcomplex), (4) reconstituted $b-c_1$ subcomplex + 0.2 μmol of antimycin A per milligram of subcomplex protein, and (5) reconstituted $b-c_1$ subcomplex + 0.15 μmol of myxothiazol per milligram of subcomplex protein).

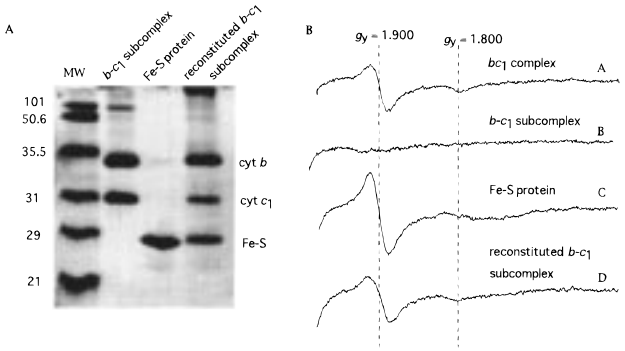

FIGURE 7: SDS−PAGE and EPR analyses of the $b-c_1$ subcomplex reconstituted with purified Fe-S protein subunit. Panel A: 4, 3.5, and 3 μg of total protein was used for $b-c_1$ subcomplex, purified Fe-S protein subunit, and reconstituted $b-c_1$ subcomplex, respectively, and the gel was stained with Coomassie Brilliant Blue. Note the appearance of the 24 kDa band corresponding to the Fe-S protein subunit. Panel B: bc_1 complex (trace A, 11 nmol), $b-c_1$ subcomplex (trace B, 14 nmol), purified Fe-S protein subunit (trace C, 10 nmol), and $b-c_1$ subcomplex (trace D, 14 nmol), reconstituted as described under Materials and Methods using 1 mol of Fe-S protein/1.3 mol of $b-c_1$ subcomplex, were reduced with 40 μM ascorbate and rapidly frozen in liquid nitrogen. The EPR spectra were taken using the following conditions: temperature, 20 K; microwave power, 5 mW; modulation amplitude, 12.5 G; modulation frequency, 100 kHz; microwave frequency, 9.4 GHz. Note the appearance of the EPR $g_y = 1.900$ and $g_x = 1.800$ signals upon reconstitution of the purified $b-c_1$ subcomplex with the Fe-S protein subunit.

DISCUSSION

In the present work, the *R. capsulatus* $b-c_1$ subcomplex lacking the Fe-S protein subunit was purified to homogeneity in large quantities, and characterized in detail. The purified $b-c_1$ subcomplex remained stable upon storage at −80 °C for over 1 year without significant loss of its reconstitutively active state. Although little is known about the interactions between the subunits of the bc_1 complex, the ability to isolate it as a physical entity indicated that cyt *b* and cyt c_1 can associate with each other to form a subcomplex in the absence of the Fe-S protein both in vivo (*17*) and in vitro. The purified $b-c_1$ subcomplex contained slightly less *b*- and *c*-type hemes in comparison to the purified bc_1 complex, and removal of the Fe-S protein subunit modified slightly the spectral characteristics of its heme b_L, leaving the E_{m7} values of its hemes b_H, b_L, and c_1 similar to those of the $b-c_1$ complex. It therefore appears that the Fe-S protein subunit

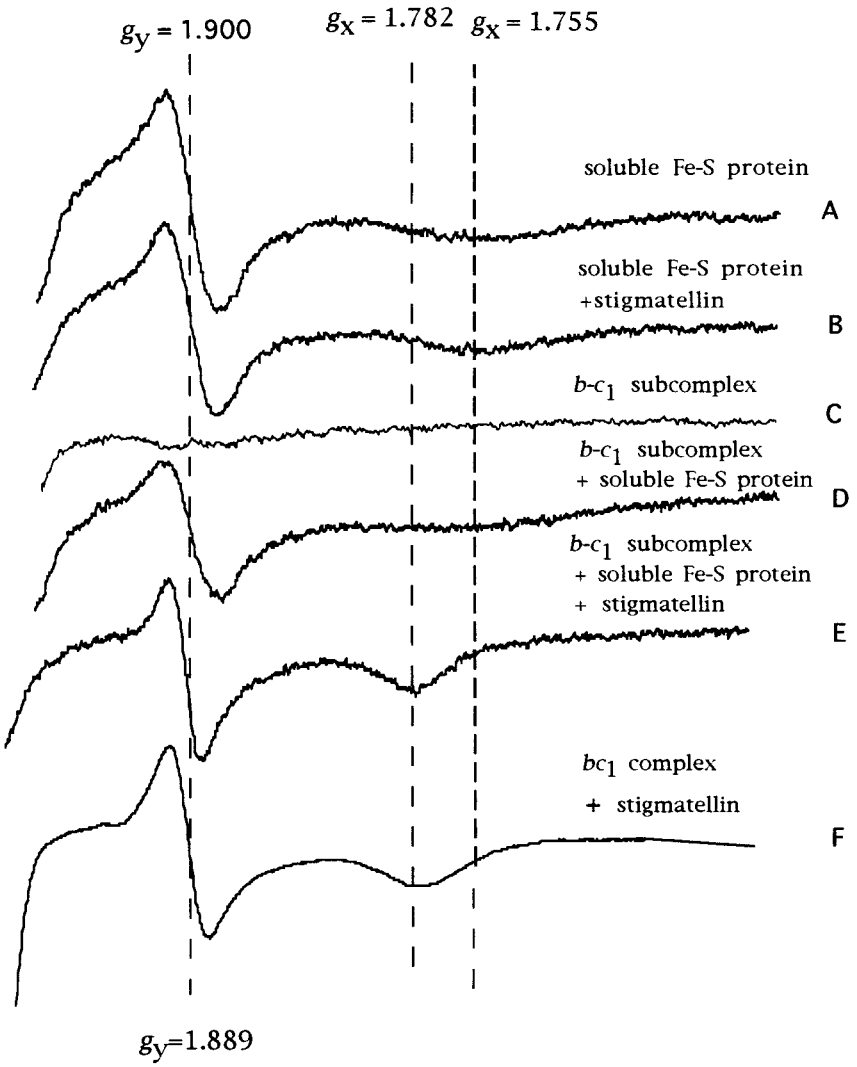

FIGURE 8: EPR spectra of the $b-c_1$ subcomplex reconstituted with a soluble derivative of the Fe-S protein subunit in the presence and absence of stigmatellin. (A) Soluble derivative of the Fe-S protein subunit (18 mg/mL); (B) soluble derivative of the Fe-S protein subunit in the presence of 30 μM stigmatellin; (C) purified $b-c_1$ subcomplex (14 nmol); (D and E) purified $b-c_1$ (14 nmol) incubated with the soluble derivative of the Fe-S protein subunit as described under Materials and Methods in the absence and presence of 30 μM stigmatellin, respectively; (F) purified bc_1 complex (10 nmol). Note the appearance of the EPR $g_x = 1.782$ signal after reconstitution of the $b-c_1$ subcomplex with the soluble derivative of the Fe-S protein subunit in the presence of stigmatellin. The EPR conditions used were as in Figure 7.

does not tightly shield cyt b_L from solvent exposure, an observation consistent with the three-dimensional structure of the bc_1 complex and with the proposed movement of the Fe-S protein subunit during Q_o site catalysis (*14*, *15*). Furthermore, as expected, the elimination of the Fe-S subunit does not affect the properties of the Q_i site in terms of its interactions with antimycin A or its ability to stabilize a semiquinone intermediate.

The effect of in vivo removal of the Fe-S protein from the bc_1 complexes varies between different species. In *R. capsulatus* (*17*), removing the [2Fe-2S] cluster has little effect on the steady-state presence of the cyt *b* and cyt c_1 subunits in chromatophore membranes. However, the *Chlamydomonas reinhardtii* mutant ac21 missing the Fe-S protein subunit of the cyt b_6f complex contains apparently 50% less cyt *f*, cyt b_6, and SU IV subunits in comparison to a wild-type strain (*42*). Equally, yeast mutants with deletion of the Fe-S protein subunit exhibit a dramatic decrease in the *cyt b* amount (*43*, *44*), and it has been suggested that the Fe-S protein is required for maintenance of the wild-type level of cyt *b* in mitochondria, while it has almost no effect on the level of the other subunits of the bc_1 complex (*43*). However, since these subcomplexes have not yet been purified either from *C. reinhardtii* or from *S. cerevisiae*, how they compare to that of *R. capsulatus* remains unknown. On the other hand, in vitro elimination of the Fe-S protein from beef mitochondrial bc_1 complex has been accomplished either by its dissociation using a detergent (*45*) or via proteolysis (*40*), and the obtained Fe-S protein-depleted mitochondrial bc_1 complexes (*46*) have properties similar to those of bacteria.

The most striking result obtained in this study is our ability to reconstitute the cyt *c* reductase activity of the $b-c_1$ subcomplex upon addition of purified wild-type Fe-S protein (Figure 9). The reconstituted complex exhibits good activity (about 25% of that of a wild-type complex), and the assay developed here is simple and sensitive, and can be readily scaled up for physical measurements requiring large amounts of sample materials, such as an EPR spectroscopy. Reconstitution of the cyt *c* reductase activity of a bc_1 complex depleted of its Fe-S protein subunit has been reported

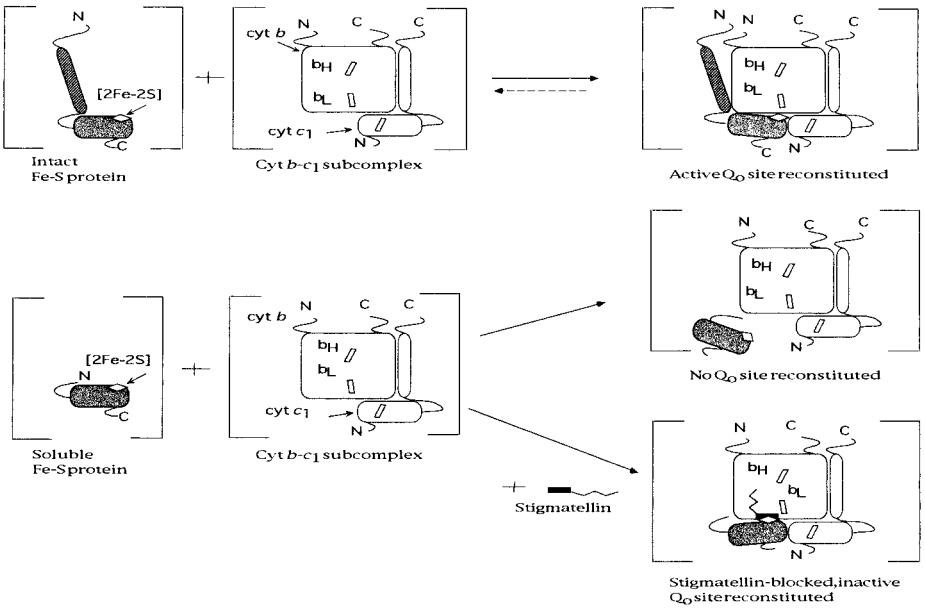

FIGURE 9: Schematic representation of the reconstitution of the $b-c_1$ subcomplex with purified intact Fe-S protein subunit, or with a soluble derivative of it lacking its first 44 amino-terminal amino acid residues containing its membrane anchor domain, in the presence and absence of stigmatellin.

previously for the beef heart mitochondrial bc_1 complex (*24*, *45*) but not for any bacterial species. This was possible because of the overproduction of the bc_1 complex and the availability of *R. capsulatus* mutants which facilitated its purification (*17*). In addition, the use of Tween 20, which inhibits reduction of cyt *c* by the Fe-S protein via the Q_o site independent oxidation of ubihydroquinone, possibly by acting as a quencher of superoxide and semiquinone radicals thus formed (1−5), rendered possible the detection of low, but specific, Q_o site dependent (i.e., sensitive to myxothiazol) cyt *c* reductase activity of the reconstituted complex.

The in vitro assay developed here was exploited to probe whether the amino-terminal anchor of the Fe-S protein subunit is essential for steady-state Q_o site catalysis. The very recent genetic (*41*) and structural (*14*, *15*) data suggest that a specific segment composed of the amino acid residues (M_{38}NASADVKA_{46} in *R. capsulatus*) located between the end of the transmembrane anchor and the beginning of the periplasmic portion of the Fe-S protein subunit may mediate its mobility proposed to be required for Q_o site catalysis. Since unlike the intact Fe-S protein subunit the soluble derivative of the Fe-S protein subunit produced by the *R. capsulatus* mutant pB:(T163F+G182S)/MT-RBC1 (*19*) could not reactivate the Q_o site of the $b-c_1$ subcomplex, it therefore appears that the first 44 amino acid residues of this subunit are required for steady-state Q_o site activity. Remarkably though, the same soluble derivative of the Fe-S protein can reassociate appropriately with the Q_o site of the $b-c_1$ subcomplex provided that stigmatellin is present. This association leads to the appearance of the characteristic EPR $g_x = 1.781$ signal observed only with a wild-type bc_1 complex. The characteristics of this EPR g_x signal are tightly correlated with the immediate environment of the [2Fe-2S] cluster (*47*), and the g_x signal detected after reconstitution is very similar to that observed with a wild-type bc_1 complex. It therefore appears that in the presence of stigmatellin the soluble form of the Fe-S protein subunit interacts with the Q_o domain of cyt *b* with a topology similar to that seen with the wild-type bc_1 complex inhibited by stigmatellin (*15*). These findings establish clearly that both the amino-terminal and the [2Fe-2S] cluster-containing carboxyl-terminal portions of the Fe-S protein need to be intact for a catalytically active Q_o site.

In summary, this work established that an inactive $b-c_1$ subcomplex, containing only the cyt *b* and cyt c_1 subunits, can be purified to homogeneity in large scale from chromatophore membranes of a *R. capsulatus* mutant lacking the Fe-S protein. The purified $b-c_1$ subcomplex has properties similar, but not identical, to those of the purified bc_1 complex, and can be reactivated for cyt *c* reductase activity upon addition of purified Fe-S protein subunit provided that the transmembrane anchor of the latter subunit is intact. The availability of a facile in vitro reconstitution assay for a simple bacterial bc_1 complex is very promising for dissecting the series of events that take place during UQH_2 oxidation at the Q_o site of the bc_1 complex.

REFERENCES

1. Trumpower, B. L., and Gennis, R. B. (1994) *Annu. Rev. Biochem. 63*, 675−716.
2. Gray, K., and Daldal, F. (1995) in *Anoxygenic Photosynthetic Bacteria* (Blankership, R. E., Madigan, M. T., and Bauer, C., Eds.) pp 747−774, Kluwer Academic Publishing, Dordrecht, The Netherlands.
3. Cramer, W. A., Martinez, S. E., Huang, D., Tae, G.-S., Everly, R. M., Heyman, J. B., Cheng, R. H., Baker, T. S., and Smith, J. L. (1994) *J. Bioenerg. Biomembr. 26*, 31−47.
4. Brandt, U., and Trumpower, B. (1994) *Crit. Rev. Biochem. Mol. Biol. 29*, 165−197.
5. Prince, R. C. (1990) in *Bacterial Photosynthesis: From Photons to Δp. The Bacteria* (Krulwich, T. A., Ed.) Vol. XII, pp 111−140, Academic Press, San Diego.
6. Daldal, F., Davidson, E., and Cheng, S. (1987) *J. Mol. Biol. 195*, 1−12.
7. Meinhardt, S. W., and Crofts, A. R. (1983) *Biochim. Biophys. Acta 723*, 219−230.
8. Robertson, D. E., Ding, H., Chelminski, P. R., Slaughter, C., Hsu, J., Moomaw, C., Tokito, M., Daldal, F., and Dutton, P. L. (1993) *Biochemistry 32*, 1310−1317.
9. Li, Y., De Vries, S., Leonard, K., and Weis, H. (1983) *FEBS Lett. 135*, 277−280.

10. Robertson, R. E., and Dutton, P. L. (1988) *Biochim. Biophys. Acta 935*, 273−291.
11. Daldal, F., Tokito, M. K., Davidson, E., and Faham, M. (1989)- *EMBO J. 8*, 3951−3961.
12. Crofts, A., Hacker, B., Barquera, B., Yun, C., and Gennis, R. (1992) *Biochim. Biophys. Acta* 1275, 61−69.
13. Brasseur, G., Saribas, S. A., and Daldal, F. (1996) *Biochim. Biophys. Acta 1275*, 61−69.
14. Xia, D., Yu, C. A., Kim, H. J.-Z., Kachurin, A. M., Zhang, L., and Deisenhofer, J. (1997) *Science 277*, 60−65.
15. Zhang, Z., Huang, L., Shulmeister, V., Chi, Y., Kim, K., Hung, L., Crofts, A., Berry, E., and Kim, S. (1998) *Nature 392*, 677−684.
16. Davidson, E., Ohnishi, T., Atta-Asafo-Adjei, E., and Daldal, F. (1992) *Biochemistry 31*, 3342−3350.
17. Davidson, E., Ohnishi, T., Tokito, M., and Daldal, F. (1992) *Biochemistry 31*, 3351−3358.
18. Gray, K., Dutton, P. L., and Daldal, F. (1994) *Biochemistry 33*, 723−733.
19. Saribas, A. S., Valkova-Valchanova, M. B., Tokito, M., and Daldal, F. (1998) *Biochemistry 37*, 8105−8114.
20. Sistrom, W. R. (1960) *J. Gen. Microbiol. 22*, 778−785.
21. Atta-Asafo-Adjei, E., and Daldal, F. (1991) *Proc. Natl. Acad. Sci. U.S.A. 88*, 492−496.
22. Gray, K., Groom, M., Myllykallio, H., Moomaw, C., Slaughter, C., and Daldal, F. (1994) *Biochemistry 33*, 3120−3127.
23. Yu, L., and Yu, C.-A. (1991) *Biochemistry 31*, 4934−4939.
24. Shimomura, Y., Nishikimi, M., and Ozawa, T. (1984) *J. Biol. Chem. 259*, 14059−14063.
25. Margoliash, E., and Frohwirt, N. (1959) *Biochem. J. 71*, 570−572.
26. Saribas, A. S., Ding, H., Dutton, P. L., and Daldal, F. (1995) *Biochemistry 34*, 16004−16012.
27. Wood, P. (1980) *Biochem. J. 192*, 761−764.
28. Berden, J. A., and Slater, E. C. (1970) *Biochim. Biophys. Acta 216*, 237−249.
29. Dutton, P. L. (1978) *Methods Enzymol. 54*, 411−435.
30. Lowry, O. H., Rosebrough, N. J., Farr, A. L., and Randall, R. J. (1951) *J. Biol. Chem. 193*, 265−275.
31. Laemmli, U. K. (1970) *Nature 227*, 680−685.
32. Towbin, H., Staehelin, T., and Gordon, J. (1979) *Proc. Natl. Acad. Sci. U.S.A. 76*, 4350−4354.
33. Ding, H., Robertson, D. E., Daldal, F., and Dutton, P. L. (1992) *Biochemistry 31*, 3144−3158.
34. Ljungdahl, P. O., Pennoyer, J. D., Robertson, D. E., and Trumpower, B. L. (1987) *Biochim. Biophys. Acta 891*, 227−241.
35. Salerno, J. C. (1984) *J. Biol. Chem. 259*, 2331−2336.
36. Rich, P. R., Jeal, A. E., Madgwich, S. A., and Mody, A. J. (1990) *Biochim. Biophys. Acta 1018*, 29−40.
37. McCurley, J. P., Miki, T., Yu, L., and Yu, C.-A. (1990) *Biochim. Biophys. Acta 1020*, 176−186.
38. van der Berg, Prince, R. C., Bashford, C. L., Takamiya, K., Bonner, W. D., and Dutton, P. L. (1979) *J. Biol. Chem. 254*, 8594−8604.
39. Howell, N., and Robertson, D. (1993) *Biochemistry 32*, 11162−11172.
40. Link, T. A., Saynovits, M., Assman, C., Iwata, S., Ohnishi, T., and von Jagow, G. (1996) *Eur. J. Biochem. 237*, 687−691.
41. Brasseur, G., Sled, V., Liebl, U., Ohnishi, T., and Daldal, F. (1997) *Biochemistry 36*, 11685−11696.
42. Lemaire, C., Girard-Bascon, J., Wollman, F.-A., and Bennoun, P. (1986) *Biochim. Biophys. Acta 851*, 229−238.
43. Crivellone, M. D., Wu, M., and Tzagoloff, A. (1988) *J. Biol. Chem. 263*, 1423−1433.
44. Ljungdahl, P. O., Beckmann, J. D., and Trumpower, B. L. (1989) *J. Biol. Chem. 264*, 3723−3733.
45. Trumpower, B. L., Edwards, C. A., and Ohnishi, T. (1980) *J. Biol. Chem. 255*, 7487−7493.
46. Gonzalez-Halphen, D., Vazquez-Acevedo, M., and Garsia-Ponce, B. (1991) *J. Biol. Chem. 266*, 3870−3876.
47. Ding, H., Mozer, C., Robertson, D., Tokito, M., Daldal, F., and Dutton, P. L. (1995) *Biochemistry 34*, 15879−15996.

BI981651Z